

# Energy Landscape of a Model Protein

Mark A. Miller and David J. Wales

*University Chemical Laboratories, Lensfield Road, Cambridge CB2 1EW, UK*

October 17, 2018

## **Abstract**

The potential energy surface of an off-lattice model protein is characterized in detail by constructing a disconnectivity graph and by examining the organisation of pathways on the surface. The results clearly reveal the frustration exhibited by this system and explain why it does not fold efficiently to the global potential energy minimum. In contrast, when the frustration is removed by constructing a ‘Gō-type’ model, the resulting graph exhibits the characteristics expected for a folding funnel.

## **1 Introduction**

The potential energy surface (PES) of an interacting system determines its structural, dynamic, and thermodynamic properties. Formally, the links between the PES and these properties are fully defined by the stationary points on the PES, its gradient (which gives the forces on the particles), and the partition function. However, it is only relatively recently that explicit connections have been sought between the overall structure of the PES, or potential energy ‘landscape’, and the behaviour of the system it describes. This

approach promises to provide insight into a number of fields, including protein folding, global optimization and glass formation.

In the present contribution we provide a global characterization of the PES for a model heteropolymer, and show how this picture explains the dynamical properties observed in previous simulations. In the original model ‘frustration’ prevents efficient relaxation to the global potential energy minimum. However, when the frustration is removed by constructing the corresponding ‘Gō-like’ model, the deep traps disappear and the resulting surface resembles a funnel. The term frustration was first used in the context of spin glasses,<sup>1</sup> where it is impossible to satisfy all favourable interactions simultaneously. Analogous effects exist in proteins:<sup>2</sup> a three-dimensional structure that brings together two mutually attractive residues may involve generating unfavourable contacts elsewhere (‘energetic frustration’), and the interconversion of two similar structures may require the disruption of existing favourable interactions (‘geometric frustration’).

The major difficulty in providing a fundamental explanation of structure, dynamics and thermodynamics in terms of the underlying potential energy surface is that the number of stationary points grows very rapidly with the size of the system.<sup>3</sup> This growth is, in fact, the basis of Levinthal’s ‘paradox’,<sup>4</sup> which points out the apparent impossibility of a protein finding its biologically active state in a random search amongst the astronomical number of available structures. Some attempts to resolve the paradox proposed a reduction in the search space from the full configuration space.<sup>5–8</sup> Although it seems unlikely that this reduction is the solution to the paradox, there is an implicit realization in such approaches that, in some way, the search is not random. In terms of the energy landscape there are two reasons for this. Firstly, conformations have different statistical weights in the thermodynamic ensemble, and secondly, they are not arranged at random in configuration space. Levinthal’s analysis assumes that the energy landscape is flat,

like a golf course with a single hole corresponding to the native state.<sup>2</sup> By constructing a simple model that includes an energetic bias towards the native structure, it can be shown that the search time on the full conformational space is dramatically reduced to physically meaningful scales.<sup>9,10</sup>

One of the first studies to consider more explicitly the organization of the energy landscape was that of Leopold, Montal, and Onuchic.<sup>11</sup> These authors proposed that the landscape of a natural protein consists of a collection of convergent kinetic pathways that lead to a unique native state which is thermodynamically the most stable. Such a landscape structure was termed a ‘folding funnel’ because it focuses the manifold misfolded states towards the correct target. This approach highlights the fundamental fallacy of the random search in Levinthal’s ‘paradox’.

Funnel theory has gained widespread acceptance through its development by Wolynes and coworkers in terms of a *free* energy landscape.<sup>2,12</sup> The funnel can be described in terms of the free energy gradient towards the native structure, and the roughness—a measure of the barrier heights between local free energy minima, which can act as kinetic traps. Folding is encouraged when the roughness is not large compared with the energy gradient. Simulations have shown that the folding ability can be measured by the ratio of the folding temperature,  $T_f$ , where the native state becomes thermodynamically the most stable, to the glass transition temperature,  $T_g$ , where the kinetics slow down dramatically because of the free energy barriers.<sup>8,13</sup>  $T_g$  is usually defined as the temperature at which the folding time passes through a certain threshold. Folding is easiest for large  $T_f/T_g$ , since the native state is then statistically populated at temperatures where it is kinetically accessible. The effect of frustration is to increase the roughness of the energy landscape relative to its gradient towards the native structure, thereby hindering relaxation to the latter.

We have recently shown<sup>14,15</sup> how a new visualization of the potential energy surface using disconnectivity graphs<sup>16</sup> reveals the features which determine relaxation of clusters to their global potential energy minimum. This approach has already been used by others to examine the energy landscape of a tetrapeptide<sup>16,17</sup> and to study the effects of conformational constraints in hexapeptides<sup>18</sup> employing an all-atom model. In the present contribution we analyse a coarse-grained representation of a larger polypeptide with 46 residues. Connected sequences of minima have been reported before for this system,<sup>19</sup> and we will show how the disconnectivity graph approach provides a clearer picture of the relation between the energy landscape and dynamics.

## 2 The Model Potential

Intermediate in detail between lattice and all-atom models of proteins are continuum bead models, in which each monomer is represented by a single bead on a chain. These off-lattice systems have received relatively little attention in terms of landscape analysis, but provide a useful medium for such an approach, since atomistic representations of proteins are computationally demanding.

Here we examine the effects of frustration in a model heteropolymer introduced by Honeycutt and Thirumalai.<sup>20,21</sup> These authors proposed a ‘metastability hypothesis’ that a polypeptide may adopt a variety of metastable folded conformations with similar structural characteristics but different energies. The particular state reached in the folding process depends on the initial conditions. We shall see that this scenario arises from frustration effects intrinsic to the model, which are not expected for a ‘good folder’.

The heteropolymer has  $N = 46$  beads linked by stiff bonds. There are three types of

bead: hydrophobic (B), hydrophilic (L), and neutral (N), and the sequence is

$$\text{B}_9\text{N}_3(\text{LB})_4\text{N}_3\text{B}_9\text{N}_3(\text{LB})_5\text{L}.$$

The potential energy is given by<sup>21</sup>

$$\begin{aligned} V = & \frac{1}{2}K_r \sum_{i=1}^{N-1} (r_{i,i+1} - r_e)^2 + \frac{1}{2}K_\theta \sum_i^{N-2} (\theta_i - \theta_e)^2 \\ & + \varepsilon \sum_i^{N-3} [A_i(1 + \cos \varphi_i) + B_i(1 + \cos 3\varphi_i)] \\ & + 4\varepsilon \sum_{i=1}^{N-2} \sum_{j=i+2}^N C_{ij} \left[ \left( \frac{\sigma}{r_{ij}} \right)^{12} - D_{ij} \left( \frac{\sigma}{r_{ij}} \right)^6 \right], \quad (1) \end{aligned}$$

where  $r_{ij}$  is the separation of beads  $i$  and  $j$ . The first term represents the bonds linking successive beads. The bond lengths were constrained at  $r_e$  in Ref. 21, but here we follow Berry et al.<sup>19</sup> by replacing these constraints with stiff springs:  $K_r = 231.2\varepsilon\sigma^{-2}$ , where  $\sigma$  and  $\varepsilon$  are the units of length and energy defined by the last term in Eq. (1). To put the energy parameter in a physical context, the value of  $\varepsilon$  suggested by Berry et al.<sup>19</sup> is 121 K, such as might be used for the van der Waals interactions between argon atoms. The second term in Eq. (1) is a sum over the bond angles,  $\theta_i$ , defined by the triplets of atomic positions  $\mathbf{r}_i$  to  $\mathbf{r}_{i+2}$ , with  $K_\theta = 20\varepsilon\text{rad}^{-2}$  and  $\theta_e = 105^\circ$ . The third term is a sum over the dihedral angles,  $\varphi_i$ , defined by the quartets  $\mathbf{r}_i$  to  $\mathbf{r}_{i+3}$ . If the quartet involves no more than one N monomer then  $A_i = B_i = 1.2$ , generating a preference for the trans conformation ( $\varphi_i = 180^\circ$ ), whereas if two or three N monomers are involved then  $A_i = 0$  and  $B_i = 0.2$ . This choice makes the three neutral segments of the chain flexible and likely to accommodate turns. The last term in Eq. (1) represents the non-bonded interactions, and  $\sigma$  is set equal to  $r_e$ . The coefficients for the various combinations of monomer types

are as follows.

$$\begin{aligned} i, j \in \text{B} & \quad C_{ij} = 1 \quad D_{ij} = 1 \\ i \in \text{L}, j \in \text{L}, \text{B} & \quad C_{ij} = \frac{2}{3} \quad D_{ij} = -1 \\ i \in \text{N}, j \in \text{L}, \text{B}, \text{N} & \quad C_{ij} = 1 \quad D_{ij} = 0, \end{aligned}$$

with  $C_{ij} = C_{ji}$  and  $D_{ij} = D_{ji}$ . Hence, hydrophobic monomers experience a mutual van der Waals attraction, and all other combinations are purely repulsive, with interactions involving a hydrophilic monomer being of longer range.

The global minimum of this system, which we call the BLN model, is a four-stranded  $\beta$ -barrel,<sup>21</sup> illustrated in Figure 1. The hydrophobic segments congregate at the core, and there are turns at the neutral segments. By cutting the sequence at these regions, Vekhter and Berry have also used this model to study the self-assembly of the  $\beta$ -barrel from the separated strands.<sup>22</sup>

### 3 Characterizing the Energy Landscape

The most important points on a PES are the minima and the transition states that connect them. A transition state is a stationary point at which the Hessian matrix has exactly one negative eigenvalue whose eigenvector corresponds to the reaction coordinate. Minima linked by higher-index saddles (the index being the number of negative Hessian eigenvalues) must also be linked by one or more true transition states of lower energy.<sup>23</sup> The pattern of stationary points and their connectivities define the topology of the PES.

### 3.1 Exploring the Landscape

All the transition states in the present work were located by eigenvector-following,<sup>24–29</sup> where the energy is maximized along one direction and simultaneously minimized in all the others. Details of our implementation have been given before.<sup>30</sup> The minima connected to a given transition state are defined by the end points of the two steepest-descent paths commencing parallel and antiparallel to the transition vector (i.e., the Hessian eigenvector whose eigenvalue is negative) at the transition state. Rather than steepest-descent minimization, we have employed a conjugate-gradient method (using only first derivatives of the potential) to calculate the pathways. This technique gives similar results, and has the advantage of being much faster. However, it is possible for conjugate-gradient minimization to converge to a stationary point of higher index than a minimum. To guard against this problem, each optimization was followed by reoptimization with eigenvector-following to a local minimum. In the majority of cases, the reoptimisation converged in a few steps, indicating that the conjugate-gradient method had indeed found a true minimum.

A number of similar approaches have been developed for systematically exploring a PES by hopping between potential wells,<sup>31–34</sup> and these can be adapted to obtain a topographical database in several ways. Here we want to explore the energy landscape thoroughly, working from the global minimum upwards. In our scheme, we commenced at the lowest-energy known minimum, and performed an eigenvector-following search for a transition state along the eigenvector with the smallest non-zero eigenvalue. Having located a transition state, the connected minima were found by evaluating the path as described above. The process was then repeated, always starting at the lowest-energy minimum found so far, and searching along eigenvectors in both directions in order of increasing eigenvalue. To enable the search to explore away from the starting minimum,

an upper limit,  $n_{\text{ev}}$ , was imposed on the number of eigenvectors to be searched from each minimum. When  $n_{\text{ev}}$  eigenvectors had been exhausted, the search moved onto the next-lowest energy minimum. We note that, even if  $n_{\text{ev}}$  is set to its maximum value of  $3N - 6$ , there is no guarantee of finding all the transition states connected to a given minimum.

The low-energy regions of the BLN model energy landscape were explored using  $n_{\text{ev}} = 10$  until 250 minima had been found. Because of the harmonic bond potential, following normal modes uphill in energy did not always lead to a transition state in a reasonable number of iterations in this system. To compensate for this problem, the value of  $n_{\text{ev}}$  was raised to 20 and the search continued until a total of 500 minima had been found. The final number of transition states was 636.

## 3.2 Visualization

A useful visual representation of a PES is provided by the disconnectivity graph of Becker and Karplus.<sup>16</sup> This technique was first introduced to interpret a structural database of the tetrapeptide isobutyryl-(ala)<sub>3</sub>-NH-methyl, produced by Czerminski and Elber,<sup>17</sup> and was subsequently applied to study the effects of conformational constraints in hexapeptides.<sup>18</sup> The method is formally expressed<sup>16</sup> in the language of graph theory, but can easily be summarized as follows.

At a given total energy,  $E$ , the minima can be grouped into disjoint sets, called ‘super-basins’, whose members are mutually accessible at that energy. In other words, each pair of minima in a super-basin are connected directly or through other minima by a path whose energy never exceeds  $E$ , but would require more energy to reach a minimum in another super-basin. At low energy there is just one super-basin—that containing the global minimum. At successively higher energies, more super-basins come into play as new minima are reached. At still higher energies, the super-basins coalesce as higher



barriers are overcome, until finally there is just one containing all the minima (provided there are no infinite barriers).

A disconnectivity graph is constructed by performing the super-basin analysis at a series of energies, plotted on a vertical scale. At each energy, a super-basin is represented by a node, with lines joining nodes in one level to their daughter nodes in the level below. The choice of the energy levels is important; too wide a spacing and no topological information is left, whilst too close a spacing produces a vertex for every transition state and hides the overall structure of the landscape. The horizontal position of the nodes is arbitrary, and can be chosen for clarity. In the resulting graph, all branches terminate at local minima, while all minima connected directly or indirectly to a node are mutually accessible at the energy of that node.

Visualization of the PES in terms of connectivity patterns between minima represents a mapping from the full configuration space onto the underlying ‘inherent structures’.<sup>35</sup> Although this approach discards information about the volume of phase space associated with each minimum, the density of minima with energy can provide a qualitative impression of the volumes associated with the various regions of the energy landscape.

Some example schematic potential energy surfaces and the corresponding disconnectivity graphs are illustrated in Figure 2. The first two examples demonstrate that a funnel-shaped landscape produces a disconnectivity graph with a single stem leading to the global minimum, from which branches sprout corresponding to local minima that are progressively cut off as the energy descends below the barriers. The contrasting nature of the funnels in Figures 2(a) and (b) is immediately discernible from the corresponding graphs, where we see that the higher barriers and lower potential energy gradient towards the global minimum in (a) produce long dangling branches in the disconnectivity graph. Figure 2(c) is qualitatively different. The PES possesses a hierarchical arrangement of

barriers, giving rise to multiple sub-branching in the graph. The strength of the disconnectivity graph in representing the topology of the PES is that it is independent of the dimensionality of the system, whereas schematic plots of the potential energy itself are restricted to one or two dimensions.

The disconnectivity graph for the low-energy regions of the BLN model landscape is shown in Figure 3, using the sample of 500 minima and 636 transition states obtained in Section 3.1. It is immediately apparent that the PES is not a single funnel. In fact, it is a good example of a rough energy landscape, with repeated splitting at successive nodes and long descending branches. A number of low-energy structures exist which are separated by high barriers. Even if the barriers were not so high, there would be little thermodynamic driving force towards the global minimum. The fact that the attractive forces are of relatively long range and non-specific character means that it is possible to construct many significantly different structures from common motifs such as the four strands in the global minimum. For example, some of the low-energy minima differ only by the relative positions of the two purely hydrophobic strands. These can register with each other in a number of positions, related visually by a parallel slide. However, such a slide would be an unlikely mechanism because all the non-bonded interactions would be disrupted at once. Instead, the shortest path between such structures typically proceeds through over ten separate rearrangements.

Other ways in which low-energy structures are related involve a reorientation of the hydrophobic strands, so that the beads which are outermost and those that come into contact in the core in Figure 1 are interchanged. Again, such a process involves many steps and a high barrier. The neutral turn regions can also adopt a number of configurations. The barriers between structures related in this way tend to be somewhat smaller, since the torsion potential is weaker in these regions.

The same structural database that is used to construct the disconnectivity graph can also be analysed in terms of ‘monotonic sequences’ of connected minima in which the potential energy decreases with every step.<sup>36,37</sup> The collection of sequences leading to a particular minimum define what we will call a monotonic sequence basin (MSB). Whilst the super-basin of the disconnectivity graph is defined at a specified energy, a monotonic sequence basin is a fixed feature of the landscape.

Berry et al.<sup>19</sup> have characterized some monotonic sequences leading to the global minimum of the BLN model. The sequences are connected by barriers that are relatively low compared with the energy gradient along the sequence, leading these authors to place the BLN model into the category of ‘structure seekers’. We note, however, that only 67 of our sample of 500 minima lie on monotonic sequences to the global minimum, so that such sequences are not representative of paths to the global minimum. Furthermore, other low-energy minima also lie at the bottom of separate monotonic sequences of comparable or even larger sets of minima. Hence, this system ‘seeks’ only a general  $\beta$ -barrel structure; consideration of the arrangement of the monotonic sequences shows that significantly different low-energy minima will be reached from different starting configurations, and interconversion of these minima will be relatively slow with little preference for any given one.

### **3.3 The Effects of Frustration**

The folding characteristics of the BLN model have recently been questioned in other studies. Guo and Brooks<sup>38</sup> used MD simulations and a histogram method to study the thermodynamics of folding. They identified a collapse transition to compact states with a peak in the specific heat, and a folding transition in terms of a similarity parameter with the global minimum. The free energy surface as a function of this parameter and the com-

pactness showed that collapse occurs before any appreciable native structure is attained, rather than the cooperative collapse and structuring expected for a good folder. Nymeyer et al.<sup>39</sup> inferred the roughness of the energy landscape from the model's thermodynamic and dynamic behaviour.<sup>40</sup> To demonstrate the effects of frustration, they compared their simulations of the BLN model with a modified version in which the frustration is largely eliminated. We now characterize the energy landscape of this modified model.

To remove the effects of frustration in the BLN model, all attractive interactions between pairs of monomers that are not in contact in the native state (global minimum) are removed. This transformation is equivalent to setting  $D_{ij} = 0$  in Eq. (1) for non-bonded pairs of hydrophobic monomers which are separated by more than  $1.167\sigma$  in the global minimum. This change increases the heterogeneity of the interactions, since it makes the attractive forces more specific. The modified potential was termed 'G $\bar{o}$ -like', following G $\bar{o}$  and collaborators, who constructed model lattice proteins by defining attractive interactions between neighbouring non-bonded monomers in an assumed ground state structure.<sup>41</sup>

Performing a survey of the energy landscape of the G $\bar{o}$ -like model as for the BLN model above produced 805 transition states linking the 500 low-lying minima. The disconnectivity graph is shown in Figure 4. The appearance is much more funnel-like, with no low-energy minima separated from the global minimum by large barriers. Relaxing the BLN global minimum with the G $\bar{o}$ -like potential actually produces the second-lowest energy structure; a similar structure differing in the orientation of one of the turns lies slightly lower. The energy range of the disconnectivity graph is a much larger proportion of the global minimum well depth than in the analogous graph for the BLN model (Figure 3). This range reflects the lower density of minima per unit energy in the G $\bar{o}$ -like system that results from the specificity of the attractive forces. The highest-energy minima in the

BLN sample were still relatively compact, whereas those for the Gō-like model showed considerable unfolding of the  $\beta$ -barrel.

The plots of energy versus shortest integrated path length to the global minimum in Figure 5 display the difference between the BLN and Gō-like energy landscapes clearly. For the BLN model there is little correlation between distance and energy, whereas for the Gō-like model the energy rises with distance, as one would expect in a funnel-like landscape.<sup>42</sup> The number of individual rearrangements along the shortest paths to the global minimum is shown for both models in Figure 6. The distribution for the BLN model is broader, with some minima lying as far as 24 steps from the global minimum, in contrast with a maximum of 15 for the Gō-like model. This reveals the greater organization of the Gō-like energy landscape into pathways converging at the global minimum.

A funnel-like interpretation for the Gō-like model is also encouraged by the changes in the average properties of the individual paths between minima, as demonstrated in Table 1. Uphill barriers are, on average, higher and downhill barriers lower for the Gō-like model, producing a steeper downhill gradient between minima. However, the funnel of the Gō-like model is far from ideal. A monotonic sequence analysis shows that only 124 of the 500 minima lie in the primary MSB, so that the relaxation from an arbitrary structure to the global minimum is likely to involve a number of uphill steps.

In simulations, Nymeyer et al.<sup>39</sup> found that the collapse from unfolded states and the formation of native structure occurred cooperatively for the Gō-like model, producing a single narrow peak in the heat capacity. They also showed that glassy dynamics, as measured by non-exponential relaxation from unfolded states, starts at temperatures just below the collapse for the BLN model, hindering the search for the native structure. In the Gō-like model, in contrast, glassy dynamics only set in below the folding temperature, where the global minimum still has a large equilibrium probability. These results

are entirely in accord with those expected from the direct characterization of the energy landscape presented here.

## 4 Conclusions

The disconnectivity graph analysis of the 3-colour, 46-bead model polypeptide reveals a frustrated energy landscape with a number of low-lying  $\beta$ -barrel structures in competition with the global potential energy minimum. Although relaxation to one of these  $\beta$ -barrel minima may be quite efficient, much longer time scales are needed for the system to reliably locate the global minimum, in agreement with previous simulations.

In contrast, when the frustration is removed by changing the potential to a G $\bar{o}$ -type model, the landscape is transformed to one where the global minimum should be located easily. The competitive low-lying minima disappear following the transformation, and the metastable minima are organised with an energy gradient towards the global minimum. Our results illustrate the utility of the disconnectivity graph approach as a tool to rationalize and predict structural, dynamic and thermodynamic behaviour from the potential energy surface.

## Acknowledgements

We are grateful to the Royal Society and the EPSRC for supporting this research, and to Dr John Rose for providing his Fortran routines for the model potential.

## References

- [1] G. Toulouse, *Comm. Phys.* **2**, 115 (1977).
- [2] J. D. Bryngelson, J. N. Onuchic, N. D. Socci and P. G. Wolynes, *Proteins: Struct., Func. and Gen.* **21**, 167 (1995).
- [3] F. H. Stillinger, *Phys. Rev. E* **59**, 48 (1999).
- [4] C. Levinthal, in *Mössbauer spectroscopy in biological systems, proceedings of a meeting held at Allerton House, Monticello, Illinois*, edited by P. DeBrunner, J. Tsiibris and E. Munck, p. 22, Urbana (1969), University of Illinois Press.
- [5] C. Levinthal, *J. Chim. Phys.* **65**, 44 (1968).
- [6] C. J. Camacho and D. Thirumalai, *Phys. Rev. Lett.* **71**, 2505 (1993).
- [7] A. Šali, E. Shakhnovich and M. Karplus, *Nature* **369**, 248 (1994).
- [8] N. D. Socci and J. N. Onuchic, *J. Chem. Phys.* **101**, 1519 (1994).
- [9] R. Zwanzig, A. Szabo and B. Bagchi, *Proc. Natl. Acad. Sci. USA* **89**, 20 (1992).
- [10] R. Zwanzig, *Proc. Natl. Acad. Sci. USA* **92**, 9801 (1995).
- [11] P. E. Leopold, M. Montal and J. N. Onuchic, *Proc. Natl. Acad. Sci. USA* **89**, 8721 (1992).
- [12] P. G. Wolynes, J. N. Onuchic and D. Thirumalai, *Science* **267**, 1619 (1995).
- [13] N. D. Socci, J. N. Onuchic and P. G. Wolynes, *J. Chem. Phys.* **104**, 5860 (1996).
- [14] D. J. Wales, M. A. Miller and T. R. Walsh, *Nature* **394**, 758 (1998).
- [15] J. P. K. Doye, M. A. Miller and D. J. Wales, *J. Chem. Phys.* **110**, 6896 (1999).

- [16] O. M. Becker and M. Karplus, *J. Chem. Phys.* **106**, 1495 (1997).
- [17] R. Czerminski and R. Elber, *J. Chem. Phys.* **92**, 5580 (1990).
- [18] Y. Levy and O. M. Becker, *Phys. Rev. Lett.* **81**, 1126 (1998).
- [19] R. S. Berry, N. Elmaci, J. P. Rose and B. Vekhter, *Proc. Natl. Acad. Sci. USA* **94**, 9520 (1997).
- [20] J. D. Honeycutt and D. Thirumalai, *Proc. Natl. Acad. Sci. USA* **87**, 3526 (1990).
- [21] J. D. Honeycutt and D. Thirumalai, *Biopolymers* **32**, 695 (1992).
- [22] B. Vekhter and R. S. Berry, *J. Chem. Phys.* **110**, 2195 (1999).
- [23] J. N. Murrell and K. J. Laidler, *J. Chem. Soc., Faraday Trans.* **64**, 371 (1968).
- [24] J. Pancíř, *Coll. Czech. Chem. Comm.* **40**, 1112 (1974).
- [25] C. J. Cerjan and W. H. Miller, *J. Chem. Phys.* **75**, 2800 (1981).
- [26] J. Simons, P. Jørgenson, H. Taylor and J. Ozment, *J. Phys. Chem.* **87**, 2745 (1983).
- [27] A. Banerjee, N. Adams, J. Simons and R. Shepard, *J. Phys. Chem.* **89**, 52 (1985).
- [28] J. Baker, *J. Comp. Chem.* **7**, 385 (1986).
- [29] D. J. Wales, *J. Chem. Phys.* **101**, 3750 (1994).
- [30] D. J. Wales and T. R. Walsh, *J. Chem. Phys.* **105**, 6957 (1996).
- [31] C. J. Tsai and K. D. Jordan, *J. Phys. Chem.* **97**, 11227 (1993).
- [32] J. P. K. Doye and D. J. Wales, *Z. Phys. D* **40**, 194 (1997).
- [33] G. T. Barkema and N. Mousseau, *Phys. Rev. Lett.* **77**, 4358 (1996).



- [34] N. Mousseau and G. T. Barkema, Phys. Rev. E **57**, 2419 (1998).
- [35] F. H. Stillinger and T. A. Weber, Phys. Rev. A **25**, 978 (1982).
- [36] R. S. Berry and R. Breitengraser-Kunz, Phys. Rev. Lett. **74**, 3951 (1995).
- [37] R. E. Kunz and R. S. Berry, J. Chem. Phys. **103**, 1904 (1995).
- [38] Z. Guo and C. L. Brooks III, Biopolymers **42**, 745 (1997).
- [39] H. Nymeyer, A. E. García and J. N. Onuchic, Proc. Natl. Acad. Sci. USA **95**, 5921 (1998).
- [40] There is some discrepancy in the details of the potential. In Ref. 39 the bond angle term of Eq. (1) is defined without the factor of  $1/2$ , but the value of  $K_\theta$  specified is *twice* that in Ref. 21. Furthermore, Ref. 39 specifies  $A_i = 1.2$  and  $B_i = 0.2$  for the dihedral term in Eq. (1) when no more than one N monomer is involved, rather than  $A_i = B_i = 1.2$ . This second discrepancy is almost certainly a typographical error, since only the trans conformation would then be locally stable. In any case, the thermodynamic results are in fairly good agreement with those of Ref. 38.
- [41] Y. Ueda, H. Taketomi and N. Gō, Biopolymers **17**, 1531 (1978).
- [42] J. P. K. Doye, M. A. Miller and D. J. Wales, J. Chem. Phys. **000**, submitted (1999).

## Tables

Table 1: Properties of individual pathways for the BLN and Gō-like models.  $b_i^{\text{up}}$  is the larger (uphill) barrier height between the two minima connected by transition state  $i$ , and  $b_i^{\text{down}}$  is the smaller (downhill) barrier.  $\Delta E_i^{\text{con}} = b_i^{\text{up}} - b_i^{\text{down}}$  is the energy difference between the two minima. The angle brackets indicate averaging over the sample of pathways. The units of energy are  $\epsilon$ .

Model	BLN	Gō-like
$\langle b^{\text{up}} \rangle_{\text{p}}$	2.59	3.07
$\langle b^{\text{down}} \rangle_{\text{p}}$	0.862	0.635
$\langle \Delta E^{\text{con}} \rangle_{\text{p}}$	1.73	2.43

## Figures

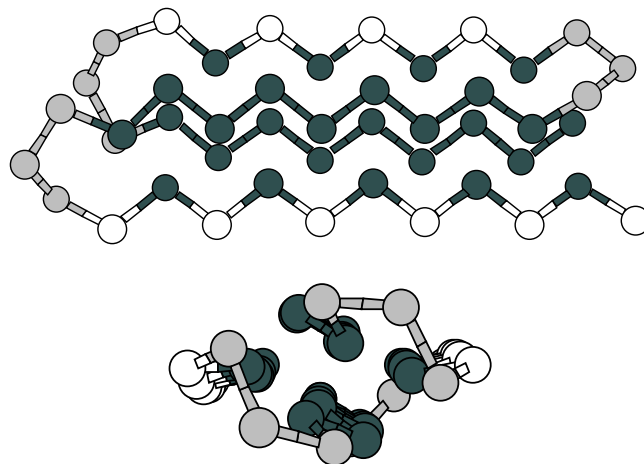


Figure 1: Side and end views of the global minimum of the BLN model. Hydrophobic, hydrophilic, and neutral beads are shaded dark grey, white and light grey, respectively.

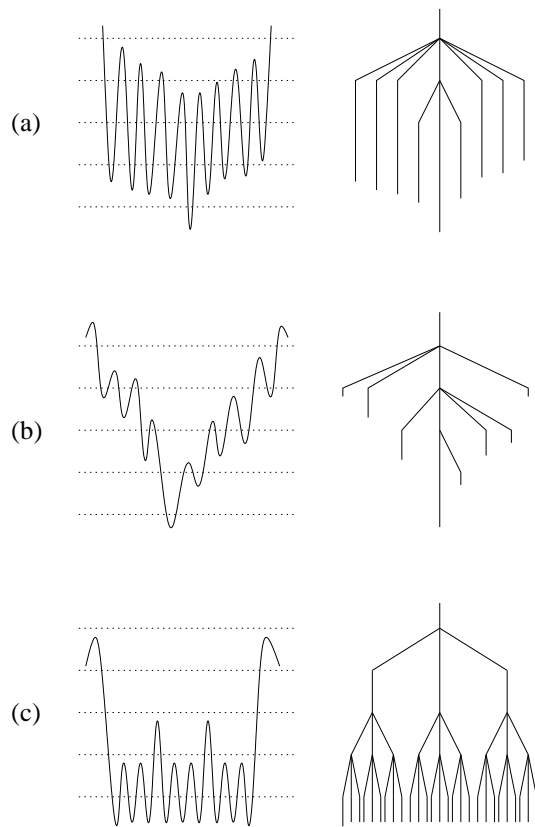


Figure 2: Schematic examples of potential energy surfaces (potential energy as a function of some generalized coordinate) and the corresponding disconnectivity graphs. In each case, the dotted lines indicate the energy levels at which the super-basin analysis has been made. (a) A gently sloping funnel with high barriers, (b) a steeper funnel with lower barriers, and (c) a 'rough' landscape.

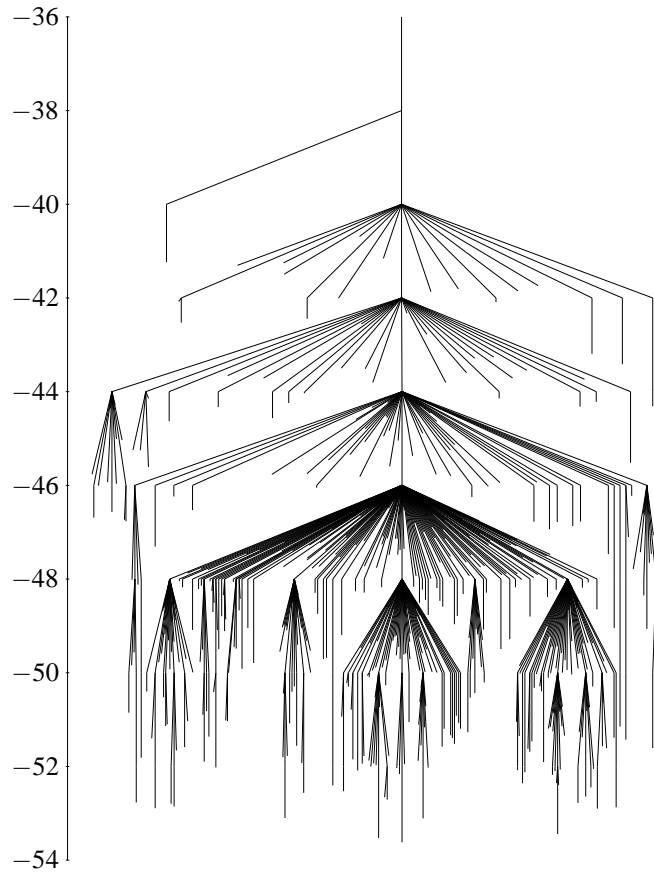


Figure 3: Disconnectivity graph for the BLN model, based on a sample of 500 minima and 636 transition states. The energy is in units of the parameter  $\varepsilon$ .

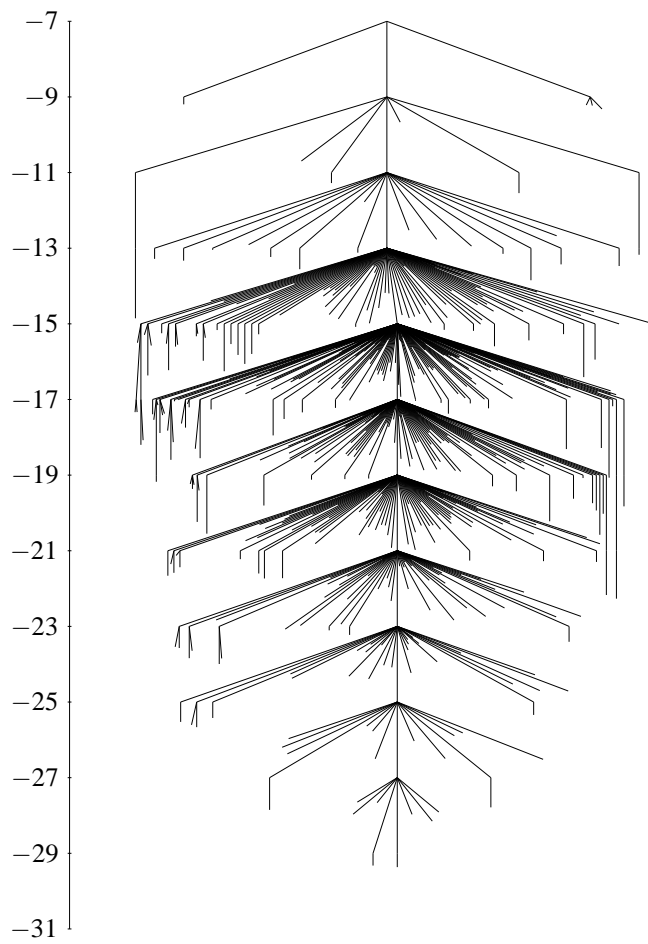


Figure 4: Disconnectivity graph for the Gō-like model, based on a sample of 500 minima and 805 transition states. The energy is in units of the parameter  $\epsilon$ .

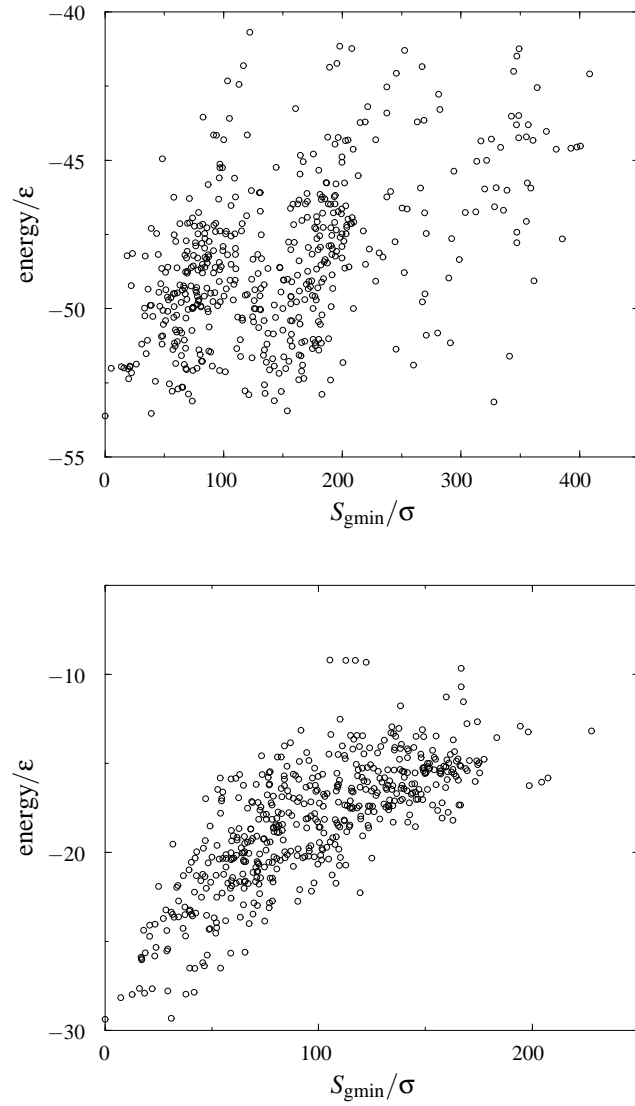


Figure 5: Energy of minima as a function of the integrated path length along the shortest path to the global minimum. Upper panel: the BLN model; lower panel: the Gō-like model.

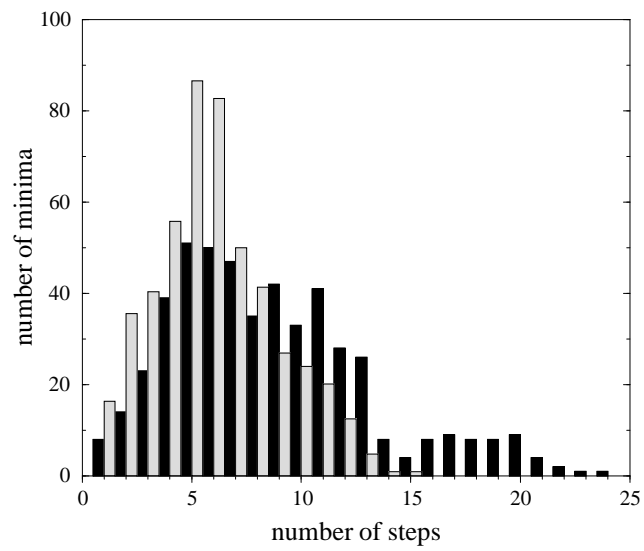


Figure 6: Distribution of the number of rearrangements along the shortest path from a given minimum to the global minimum for the BLN model (black) and the Gō-like model (grey).